21st International Conference Man and Working Environment
SEMSIE
Safety Engineering & Management – Science, Industry, Education

ORIGINAL SCIENTIFIC PAPER

DOI: 10.46793/SEMSIE25.043G

BOŠTJAN GENORIO[1]
IVO BARDAROV[2]
PEDRO MARTINS[3]
DESISLAVA YORDANOVA APOSTOLOVA[4]

[1,2,4]University of Ljubljana, Faculty of Chemistry and Chemical Technology, Slovenia
[3]Department of Materials Chemistry National Institute of Chemistry, Ljubljana, Slovenia

[1]bostjan.genorio@fkkt.uni-lj.si
[2]ivo.bardarov@fkkt.uni-lj.si
[3]pedro.martins@ki.si
[4]desislava.apostolova@fkkt.uni-lj.si

UPCYCLED CARBON BLACK AS AN ELECTROCATALYST FOR HYDROGEN PEROXIDE GENERATION

Abstract: *Carbon black is used in many industries due to its versatility and low cost. In this work, a cost-effective and scalable method for upcycling carbon black to carbon black flash graphene (CB-FG) using the fast flash joule heating (FJH) technique is presented. Extensive morphological, structural, spectroscopic and chemical analyses show that the resulting CB-FG exhibits lamellar morphology, low oxygen content, and a turbostratic graphitic structure. These properties underpin its excellent electrochemical performance in the two-electron oxygen reduction reaction ($2e^-$ ORR) for the electrosynthesis of hydrogen peroxide (H_2O_2). CB-FG shows up to 95% selectivity and high activity in 0.1 M KOH, making it a strong candidate for practical H_2O_2 electrosynthesis applications. Overall, this study advances the development of sustainable, upcycled electrocatalysts for H_2O_2 production and contributes to a circular economy and global sustainability initiatives.*

Keywords: Flash graphene; Flash Joule heating; upcycling; electrochemical synthesis; sustainability

ORCID iDs:	Boštjan Genorio	https://orcid.org/0000-0002-0714-3472
	Ivo Bardarov	https://orcid.org/0000-0003-1352-4834
	Pedro Martins	https://orcid.org/0000-0002-7078-0378
	Desislava Yordanova Apostolova	https://orcid.org/0009-0002-9760-2229

INTRODUCTION

Hydrogen peroxide (H_2O_2) is an important industrial chemical whose market is expected to reach USD 4.5 billion by 2032 (Wen et al., 2024) . Currently, over 95% of global production is manufactured using the centralized, multi-step anthraquinone process, which includes organic solvents, anthraquinone derivatives, Pd-based catalysts, and energy-intensive purification steps (Campos-Martin et al., 2006). Alternatively, H_2O_2 can be produced via direct synthesis from hydrogen and oxygen, but it is considered dangerous and unsustainable.

A cleaner, safer, and more sustainable alternative to the production of hydrogen peroxide is the direct electrochemical synthesis from water and oxygen via the two-electron oxygen reduction reaction ($2e^-$ ORR). This method has attracted considerable attention due to its potential for decentralized, on-demand H_2O_2 production (Farinazzo Bergamo Dias Martins et al., 2023). However, its commercialization is hindered by the lack of efficient and selective electrocatalysts. Various catalysts have been investigated, including platinum group metals (PGMs), their alloys, and transition metals such as Co (Cui et al., 2023), Fe (Zhang et al., 2023) and Ni (Nosan et al., 2023). While these materials exhibit high activity and H_2O_2 selectivity of up to 98%, their high cost, scarcity, and susceptibility to poisoning and deactivation limit their wide application. This has led to a growing interest in carbon-based nanomaterials, which offer a promising combination of activity, selectivity, and stability for $2e^-$ ORR (Bardarov et al., 2024). In particular, oxidized carbon materials have been shown to perform well in H_2O_2 electrosynthesis (Lu et al., 2018). However, many carbon electrocatalysts require complex and time-consuming synthesis routes, limiting their scalability and commercial viability. In line with sustainable and cost-effective approaches, we explored the use of upcycled, low-cost carbon materials. Specifically, we have focused on carbon black as a precursor for the development of an efficient electrocatalyst for H_2O_2 production.

Carbon black is a fine powder consisting of nanoscale amorphous carbon particles, usually produced by the incomplete combustion of various precursors. It is often used as a reinforcing filler in rubber composites to increase durability and wear resistance. In addition, carbon black serves as a black pigment in inks, paints, and plastics, providing color depth as well as UV protection. Its high surface-to-volume ratio and good electrical conductivity also make it valuable in electronics and energy storage and conversion technology. In contrast, graphene-based carbon materials offer superior properties, such as exceptional mechanical strength and one of the highest known electrical conductivities. However, their commercial use has been limited by high production costs, scalability issues, environmental concerns and inconsistent product quality associated with conventional synthesis methods (Wyss, Beckham, et al., 2021). An important advance was made in 2019 when Tour and colleagues demonstrated that various

carbon sources can be rapidly converted to turbostratic flash graphene (FG) using flash Joule heating (FJH) (Luong et al., 2020). In this context, the upcycling of carbon black into graphene-like derivatives represents a promising route to both scalable graphene production and the development of efficient electrocatalysts for H_2O_2 electrosynthesis. This motivation builds on our previous work where we successfully upcycled carbon fiber composites (CFCs) into highly efficient electrocatalysts for H_2O_2 generation using the FJH method (Bardarov et al., 2025).

Flash Joule Heating (FJH) is a simple, cost-effective bottom-up method for producing graphene. It involves passing a high-energy electrical pulse through a partially conductive sample, causing the temperature to rise to over 3000 K within milliseconds. This extreme thermal shock causes the sample to atomize and reorganize into a thermodynamically stable turbostratic graphite structure during rapid cooling, resulting in a product with a carbon content of up to 99% by weight. The ultra-fast cooling is crucial as it prevents the formation of the Bernal stacking (AB) typical of graphite (Wyss, Beckham, et al., 2021). Instead, the resulting turbostratic graphene exhibits a rotational disorder between the layers, leading to a larger interlayer spacing and a weaker van der Waals interaction. These weaker π-π stacking interactions make the structure easier to exfoliate and disperse into individual layers of the so-called flash graphene (FG) (Wyss, Wang, et al., 2021). This improved processability makes FG particularly attractive for various applications, especially for electrocatalysis for the oxygen reduction reaction (ORR) (Bardarov et al., 2025) and the hydrogen evolution reaction (HER) (Wyss et al., 2022) .

This article presents a novel approach for the upcycling of carbon black (CB) into high-quality flash graphene (FG) using flash Joule heating (FJH). The resulting material - carbon black-derived flash graphene (CB-FG) - shows excellent electrocatalytic performance for the $2e^-$ ORR and exhibits high activity and selectivity for electrochemical H_2O_2 production. This cost-effective, scalable method not only upcycles CB, but also provides a sustainable route to advanced carbon materials with great potential for clean energy and green chemical synthesis applications.

MATERIALS AND METHODS

Synthesis of Carbon Black Flash Graphene (CB-FG)

Carbon black flash graphene (CB-FG) was synthesized from carbon black (Ketjenblack EC-300J). The high conductivity of CB makes it ideal for flash Joule heating (FJH), eliminating the need for conductive additives. Typically, 200 mg of CB yields ~80% CB-FG. Weight loss results from volatile release during pretreatment and physical loss during flashing. A custom lab-scale FJH system was built to produce <1 g batches. For safety, the setup was enclosed in a grounded metal box inside a ventilated fume hood. The control unit, including the charger and emergency discharge circuit, was placed in a safe distance. Experiments were conducted with the sash closed and appropriate light shielding. A voltmeter and signal light confirmed capacitor discharge before sample retrieval. The experimental setup includes a 168 mF capacitor bank (400 V), charged via a half-wave rectifier with a current-limiting resistor. A thyristor switch delivers pulse currents up to 16 kA for 10 ms, controlled by an Arduino. An oscilloscope tracks voltage and current in real time. A 12 VAC, 20+ A power supply is used for pretreatment, which removes volatiles and prevents pressure buildup.

Scanning Electron Microscopy (SEM) and Transmission Electron Microscopy (TEM) analysis

Material morphology was analysed using a Zeiss ULTRA Plus field emission SEM (FE-SEM). Samples were mounted on conductive carbon tape affixed to an aluminium stub and imaged at 2 kV with an SE2 detector at a 5.5 mm working distance. TEM analysis of CB-FG was conducted using a JEOL ARM 200 CF microscope at 80 kV. For TEM, CB-FG was dispersed onto a carbon-coated copper grid.

X-ray photoelectron spectroscopy (XPS)

XPS analyses were performed using a Versa Probe 3 AD system (PHI, Chanhassen, USA) equipped with a monochromatic Al Kα X-ray source, operating at 15 kV accelerating voltage and 13.3 mA emission current. Powder samples were mounted on double-sided Scotch tape and placed at the center of the XPS holder. Spectra were collected over a 200 × 200 μm area with the charge neutralizer enabled. Survey scans were acquired using a pass energy of 224 eV and a step size of 0.8 eV, while high-resolution spectra were recorded with a pass energy of 27 eV and a step size of 0.1 eV. To ensure a strong signal-to-noise ratio, each spectrum was averaged over a minimum of 10 sweeps. Energy scale calibration and charge correction were performed by referencing the C=C component of the C 1s peak at a binding energy (BE) of 284.5 eV. Spectral deconvolution was carried out using MultiPak 9.9.1 and CasaXPS software, with Shirley background subtraction applied to all spectra.

Powder X-ray diffraction (XRD)

X-ray diffraction (XRD) measurements were performed using a PANalytical X'Pert PRO MPD diffractometer equipped with Cu $K\alpha 1$ radiation (λ = 1.5406 Å). Data were collected over a 2θ range of 10°–60° with a step size of 0.034° per 100 seconds, using a fully opened X'Celerator detector. Samples were mounted on a zero-background silicon holder.

Raman spectroscopy

Raman spectra were acquired using a WITec Alpha 300 RAS system equipped with a 532 nm laser (P = 5 mW), a 50× objective with a numerical aperture; NA = 0.8, and an integration time of 1 second. The reported spectra represent averaged data obtained from large-area mapping over a 50 × 40 μm region, sampled at a resolution of 100 × 80 pixels.

Electrode preparation and electrochemical measurements

Electrochemical measurements of CB-FG were performed using a rotating ring-disk electrode (RRDE, AFE6R2GCAU, Pine Research) with a GC disk (0.2376 cm²) and a gold ring (0.2356 cm²). The electrode was polished with 9 µm and 0.05 µm diamond paste (MetaDi™ Supreme, Buehler) and rinsed with ultrapure water (18.2 MΩ·cm, Milli-Q). CB-FG ink (2.376 mg·mL^{-1}) was prepared by dispersing 17.2 mg of CB-FG in 5.79 mL ultrapure water, 1.39 mL IPA (99.999%, Sigma-Aldrich), and 61.88 µL PFSA ionomer (Aquivion D98-25BS, 25% in water, Sigma-Aldrich), followed by 1 h of sonication. A 10 µL aliquot (100 µg·cm^{-2} loading) was drop-cast onto the GC disk and dried under ambient conditions. RRDE experiments were conducted with a WaveVortex10 rotator and a PalmSens4 bi-potentiostat, using Ag/AgCl/3 M NaCl as the reference, a glassy carbon rod as the counter electrode, and 0.1 M $HClO_4$, 0.5 M NaCl, and 0.1 M KOH as the electrolyte. Collection efficiencies were determined prior to measurements using 10 mM $[Fe(CN)_6]^{3-}$ in 0.1 M KOH at 1600 rpm and 50 mV·s^{-1}: $N = 0.383$ for the Au ring.

RESULTS AND DISCUSSION

CB-FG was synthesized via a two-step process involving preheating and FJH on a device presented in **Figure 1 (a) and 1 (b)**. The method was optimized for consistent material quality. In the first step, compressed carbon black (**Figure 1 (c)**) was pretreated by resistance heating at 20 A for 5 seconds. In the second step, a 200 ms high-current pulse (up to 1000 A) was applied to furnish carbon black flash graphene (CB-FG) as shown in **Figure 1 (d)**. CB-FG shows visible morphological changes when compared to CB precursor.

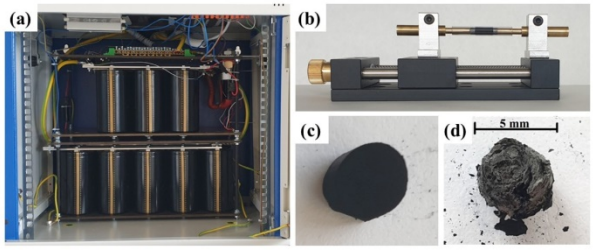

Figure 1. ***(a)*** *Flash Joule heating (FJH) setup showing the visible capacitor bank.* ***(b)*** *Sample holder with mounted precursor prior to preheating and FJH.* ***(c)*** *Compressed carbon black precursor before treatment.* ***(d)*** *Resulting carbon black flash graphene (CB-FG) after preheating and FJH.*

The morphology of the synthesized product was further investigated using electron microscopy (**Figure 2**). Scanning electron microscopy (SEM) revealed that the CB-FG exhibits a characteristic layered morphology, indicative of a turbostratic graphitic structure (**Figure 2 (a)**). The primary objective of transforming the amorphous, particulate morphology of carbon black (CB) into a graphitic-like structure was successfully confirmed by SEM analysis. Additionally, transmission electron microscopy (TEM) provided further evidence of this transformation, showing that the initially amorphous carbon black structure had been converted into a multilayered, turbostratic graphitic arrangement with noticeable wrinkling (**Figure 2 (b)**). The extremely rapid heating and cooling rates - on the order of milliseconds - impeded the formation of a fully crystalline graphitic structure typical of hexagonal graphite. Instead, these conditions favoured the development of short-range ordering and the emergence of curved, turbostratic graphitic layers. Such a structure is advantageous for subsequent material processing and facilitates easier exfoliation during the preparation of graphene-based electrocatalyst inks.

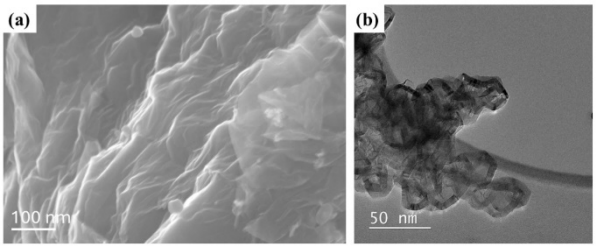

Figure 2. *Electron microscopy characterization of carbon black-derived flash graphene (CB-FG).* ***(a)*** *SEM image of CB-FG, illustrating its surface morphology, and* ***(b)*** *TEM image of CB-FG, revealing its internal microstructure.*

The structure was further characterized using X-ray diffraction (XRD) and Raman spectroscopy. XRD analysis revealed a highly crystalline structure, as evidenced by relatively sharp diffraction peaks. Notably, reflections corresponding to the (002), (101), and (004) crystal planes appear at 25.9°, 42.6°, and 53.5°, respectively (**Figure 3 (a)**). A minor peak at 35.7° suggests the presence of a small amount of SiC (111) as an impurity coming from a glass tube where flashing occurred. Focusing on the prominent (002) diffraction peak, the interlayer spacing $d_{(002)}$ was calculated to be 0.343 nm, which is larger than the typical value of 0.335 nm for highly crystalline hexagonal graphite with ABAB (Bernal) stacking. This increased interlayer distance is characteristic of a turbostratic, misaligned graphitic structure, corroborating observations made in TEM images.

Further confirmation of the turbostratic nature was obtained through Raman spectroscopy. The CB-FG sample exhibits distinct and sharper D and G peaks at 1337 cm^{-1} and 1570 cm^{-1}, respectively (**Figure 3 (b)**), in contrast to the broad and diffuse features typically observed in amorphous carbon black (CB) precursors. Additionally, prominent 2D, D+G, and 2D′ peaks are observed at 2700 cm^{-1}, 2914 cm^{-1}, and 3204 cm^{-1}, respectively, indicating a graphitic structure with multiple layers. To gain deeper insight into the structural order, we evaluated the I_D/I_G and I_{2D}/I_G intensity ratios. The I_D/I_G ratio of 0.67 suggests moderate structural disorder or a high density of edge sites, both consistent with a turbostratic morphology. The I_{2D}/I_G ratio of 0.68 further supports the formation of a few-layer, turbostratic graphene-like material, in agreement with the TEM and XRD findings.

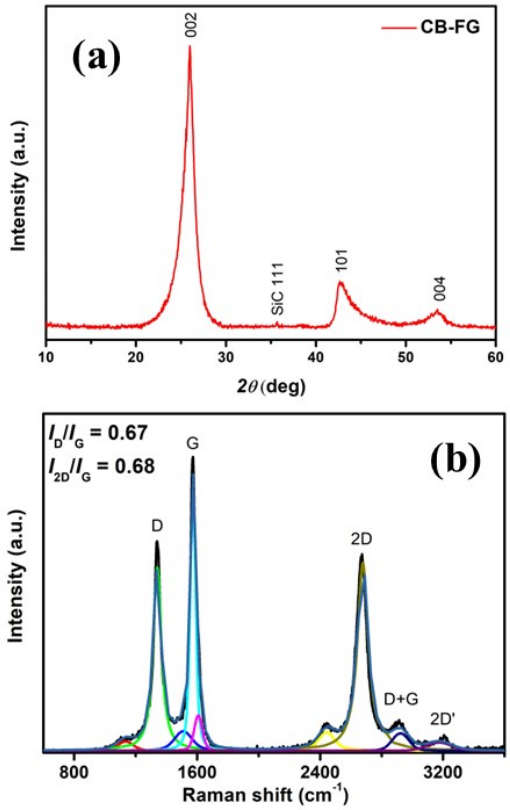

Figure 3. *Structural characterization of CB-FG.* ***(a)*** *XRD pattern of CB-FG, indicating high crystallinity.* ***(b)*** *Fitted Raman spectrum of CB-FG, highlighting the I_D/I_G and I_{2D}/I_G intensity ratios.*

To evaluate the chemical composition and surface functionalities of the synthesized material, X-ray photoelectron spectroscopy (XPS) analysis was performed. The survey spectrum revealed the presence of only two elements: carbon (99 at.%) and oxygen (1 at.%), as shown in **Figure 4 (a)**. This result demonstrates that the FJH process produces a highly pure carbonaceous product with a remarkably low concentration of oxygen-containing surface groups, indicating effective graphitization and minimal oxidation.

To gain deeper insight into the nature and distribution of surface functionalities, high-resolution C 1s core-level spectra were acquired and deconvoluted into five distinct components. The deconvolution identified peaks corresponding to: *sp²*-hybridized carbon at 284.5 eV, *sp³*-hybridized carbon at 285.0 eV, –C–O (epoxy or hydroxyl) at 286.5 eV, –C=O (carbonyl) at 288.0 eV, and –COO (carboxyl) at 289.3 eV, as illustrated in **Figure 4 (b)**. Quantitative analysis of the fitted peaks further supports the graphene-like nature of the material, with *sp²* carbon accounting for 94 at.% of the total signal, while only 1.3 at.% is attributed to *sp³*-hybridized carbon. The remaining oxygen-containing groups include –C–O (2.4 at.%), –C=O (1.0 at.%), and –COO (1.3 at.%), indicating the presence of minor surface oxidation.

These oxygen functionalities, although present in low concentrations, may play a significant role in the material's performance as an electrocatalyst. Specifically, surface-bound oxygen species can enhance electrocatalytic activity by modifying the electronic structure and increasing the density of active sites. However, they may also pose a disadvantage by potentially reducing the chemical and structural stability of the catalyst during prolonged oxygen reduction reaction (ORR) (Pavko et al., 2023).

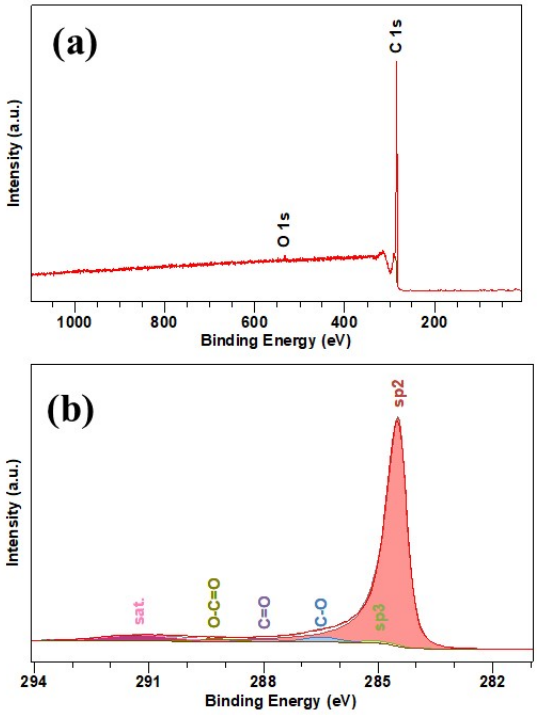

Figure 4. *XPS spectra of CB-FC.* ***(a)*** *survey spectrum and* ***(b)*** *fitted C 1s core level.*

In the final stage, the synthesized CB-FG was evaluated for its electrocatalytic performance toward the two-electron oxygen reduction reaction (2e⁻ ORR) in acidic (0.1 M $HClO_4$), neutral (0.5 M NaCl), and alkaline (0.1 M KOH) electrolytes. Carbon-based materials are known to favour the 2e⁻ ORR pathway, selectively producing hydrogen peroxide (H_2O_2) in acidic and neutral media, and hydroperoxide anions (HO_2^-) in alkaline conditions, while suppressing the competing four-electron pathway that reduces O_2 to water. Notably, in alkaline media, the pKa of H_2O_2 is 11.6, indicating that HO_2^- is the predominant species in alkaline electrolyte (**Eqn. (1)**).

$$O_2 + H_2O + 2e^- \rightarrow HO_2^- + OH^- \qquad \textbf{(1)}$$

ORR polarization curves (**Figure 5(a)** – lower graph) revealed that CB-FG exhibits the highest activity in alkaline electrolyte, moderate activity in neutral, and the lowest in acidic media. Specifically, the overpotential in neutral conditions was approximately 290 mV higher than in alkaline media at a current density of −0.1 mA, while the acidic medium required significantly higher overpotentials (681 mV higher than in alkaline media at a current density of −0.1 mA). The enhanced activity in alkaline media is attributed to reaction mechanism and the material's turbostratic structure and excellent electrical conductivity, both of

which facilitate efficient charge transfer. Rotating ring-disk electrode (RRDE) measurements were used to assess 2e$^-$ ORR selectivity (**Figure 5 (a)** – upper graph and **Figure 5 (b)**). CB-FG demonstrated over 90% selectivity in the range of 0.3–0.6 V vs. RHE in alkaline conditions, over 60% in the 0.0–0.3 V range in neutral electrolyte, and a maximum 10% at ~0.2 V in acidic conditions. The superior selectivity in alkaline media is linked to the presence of oxygen-containing functional groups and the increased interlayer spacing characteristic of turbostratic graphene, which create catalytically active sites in alkaline favourable for the 2e$^-$ ORR, as supported by density functional theory (DFT) studies (Perazzolo et al., 2015).

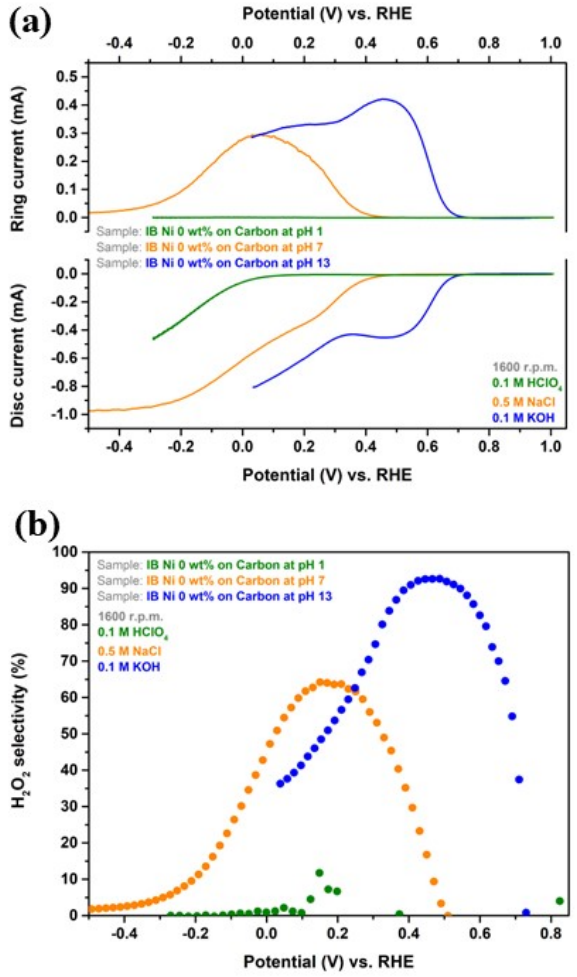

Figure 5. *Electrochemical characterization of CB-FG using RRDE. (a) Linear sweep voltammetry (LSV) polarization curves for the oxygen reduction reaction (ORR) recorded using a rotating ring-disk electrode (RRDE) setup. Simultaneous formation and detection of H_2O_2 species (HO_2^- in alkaline media) was achieved via the disk (formation - lower curves) and ring (detection - upper curves) electrodes. Measurements were conducted in O_2-saturated 0.1 M $HClO_4$, 0.5 M NaCl, and 0.1 M KOH electrolytes at a scan rate of 50 mV s^{-1} and a rotation speed of 1600 rpm. (b) H_2O_2 selectivity of CB-FG, calculated from the corresponding polarization curves, is presented for each electrolyte. The data illustrate the material's efficiency toward the 2e$^-$ ORR pathway across acidic, neutral, and alkaline environments.*

CONCLUSIONS

FJH has emerged as a highly efficient and scalable method for upcycling CB into CB-FG, effectively addressing many limitations of conventional graphene synthesis techniques. The process aligns with green chemistry principles, offering a sustainable route for transforming low-value materials into high-value, high-performance carbon nanomaterials. Electron microscopy reveals that CB-FG exhibits a lamellar-like morphology and a graphitic structure with a high specific surface area. Structurally, CB-FG possesses a turbostratic graphitic structure, as confirmed by Raman spectroscopy and XRD. XPS further shows that the material consists of 99 at.% carbon and only 1 at.% oxygen, highlighting the high purity achieved through the FJH process.

These combined structural and chemical characteristics underpin the material's excellent electrocatalytic performance in the 2e$^-$ ORR. In alkaline electrolytes, CB-FG achieves up to 95% selectivity for hydrogen peroxide production along with moderate catalytic activity. However, its selectivity and activity decrease in neutral conditions and are notably lower in acidic environments. Beyond its promising electrocatalytic potential, this approach also exemplifies how innovative materials science can contribute to circular economy goals and help mitigate environmental challenges through efficient upcycling strategies. Overall, CB-FG combines high catalytic activity with near-ideal selectivity in alkaline media, positioning it as a strong candidate for sustainable and efficient H_2O_2 electrosynthesis.

ACKNOWLEDGEMENTS

The financial support of the Slovenian Research and Innovation Agency (ARIS) through grants P2-0423, P1-0447, J7-4636, J2-50086, and J7-50227 is gratefully acknowledged.

REFERENCES

Bardarov, I., Apostolova, D. Y., Martins, P., Angelov, I., Ruiz-Zepeda, F., Jerman, I., Dular, M., Strmčnik, D., & Genorio, B. (2025). *Flash graphene from carbon fiber composites: A sustainable and high-performance electrocatalyst for hydrogen peroxide production.* Electrochimica Acta, 517. https://doi.org/10.1016/j.electacta.2025.145754

Bardarov, I., Apostolova, D. Y., Mathew, M. M., Nosan, M., Dias Martins, P. F. B., & Genorio, B. (2024). *Flash Graphene: a Sustainable Prospect for Electrocatalysis*. Acta Chimica Slovenica, 71(4), 541–557. https://doi.org/10.17344/acsi.2024.8794

Campos-Martin, J. M., Blanco-Brieva, G., & Fierro, J. L. G. (2006). *Hydrogen peroxide synthesis: An outlook beyond the anthraquinone process*. Angewandte Chemie - International Edition, 45(42), 6962–6984. https://doi.org/10.1002/anie.200503779

Cui, X., Zhong, L., Zhao, X., Xie, J., He, D., Yang, X., Lin, K., Wang, H., & Niu, L. (2023). *Ultrafine Co nanoparticles confined in nitrogen-doped carbon toward two-electron*

oxygen reduction reaction for H_2O_2 electrosynthesis in acidic media. Chinese Chemical Letters, 34(11). https://doi.org/10.1016/j.cclet.2023.108291

Farinazzo Bergamo Dias Martins, P., Plazl, I., Strmcnik, D., & Genorio, B. (2023). *Prospect of microfluidic devices for on-site electrochemical production of hydrogen peroxide*. In Current Opinion in Electrochemistry (Vol. 38). Elsevier B.V. https://doi.org/10.1016/j.coelec.2023.101223

Lu, Z., Chen, G., Siahrostami, S., Chen, Z., Liu, K., Xie, J., Liao, L., Wu, T., Lin, Di., Liu, Y., Jaramillo, T. F., Nørskov, J. K., & Cui, Y. (2018). *High-efficiency oxygen reduction to hydrogen peroxide catalysed by oxidized carbon materials.* Nature Catalysis, 1(2), 156–162. https://doi.org/10.1038/s41929-017-0017-x

Luong, D. X., Bets, K. V., Algozeeb, W. A., Stanford, M. G., Kittrell, C., Chen, W., Salvatierra, R. V., Ren, M., McHugh, E. A., Advincula, P. A., Wang, Z., Bhatt, M., Guo, H., Mancevski, V., Shahsavari, R., Yakobson, B. I., & Tour, J. M. (2020). *Gram-scale bottom-up flash graphene synthesis*. Nature, 577(7792), 647–651. https://doi.org/10.1038/s41586-020-1938-0

Nosan, M., Strmčnik, D., Brusko, V., Kirsanova, M., Finšgar, M., Dimiev, A. M., & Genorio, B. (2023). *Correlating nickel functionalities to selectivity for hydrogen peroxide electrosynthesis*. Sustainable Energy and Fuels, 7(9), 2270–2278. https://doi.org/10.1039/d3se00139c

Pavko, L., Gatalo, M., Đukić, T., Ruiz-Zepeda, F., Surca, A. K., Šala, M., Maselj, N., Jovanovič, P., Bele, M., Finšgar, M., Genorio, B., Hodnik, N., & Gaberšček, M. (2023). *Correlating oxygen functionalities and electrochemical durability of carbon supports for electrocatalysts*. Carbon, 215. https://doi.org/10.1016/j.carbon.2023.118458

Perazzolo, V., Durante, C., Pilot, R., Paduano, A., Zheng, J., Rizzi, G. A., Martucci, A., Granozzi, G., & Gennaro, A. (2015). *Nitrogen and sulfur doped mesoporous carbon as metal-free electrocatalysts for the in situ production of hydrogen peroxide*. Carbon, 95, 949–963. https://doi.org/10.1016/j.carbon.2015.09.002

Wen, Y., Feng, Y., Wei, J., Zhang, T., Cai, C., Sun, J., Qian, X., & Zhao, Y. (2024). *Photovoltaic-driven stable electrosynthesis of H2O2 in simulated seawater and its disinfection application*. Chemical Science. https://doi.org/10.1039/d4sc05909c

Wyss, K. M., Beckham, J. L., Chen, W., Luong, D. X., Hundi, P., Raghuraman, S., Shahsavari, R., & Tour, J. M. (2021). *Converting plastic waste pyrolysis ash into flash graphene*. Carbon, 174, 430–438. https://doi.org/10.1016/j.carbon.2020.12.063

Wyss, K. M., Chen, W., Beckham, J. L., Savas, P. E., & Tour, J. M. (2022). *Holey and Wrinkled Flash Graphene from Mixed Plastic Waste*. ACS Nano, 16(5), 7804–7815. https://doi.org/10.1021/acsnano.2c00379

Wyss, K. M., Wang, Z., Alemany, L. B., Kittrell, C., & Tour, J. M. (2021). *Bulk Production of Any Ratio 12C:13C Turbostratic Flash Graphene and Its Unusual Spectroscopic Characteristics*. ACS Nano, 15(6), 10542–10552. https://doi.org/10.1021/acsnano.1c03197

Zhang, Q., Zheng, L., Gu, F., Wu, J., Gao, J., Zhang, Y. C., & Zhu, X. D. (2023). *Recent advances in single-atom catalysts for acidic electrochemical oxygen reduction to hydrogen peroxide*. In Nano Energy (Vol. 116). Elsevier Ltd. https://doi.org/10.1016/j.nanoen.2023.108798